Available online at www.sciencedirect.com
SCIENCE DIRECT®
Journal of Nuclear Materials 336 (2005) 11–21
journal of nuclear materials
www.elsevier.com/locate/jnucmat

Numerical evaluation of the dislocation loop bias

V.I. Dubinko *, A.S. Abyzov, A.A. Turkin

NSC KIPT, Kharkov 61108, Ukraine

Received 1 March 2004; accepted 7 July 2004

Abstract

We have performed numerical calculation of the capture efficiency of a dislocation loop in a finite toroidal reservoir, which is a more appropriate model for a dislocation loop than a spherical or cylindrical reservoir adopted in the previous models. It allows a direct evaluation of the capture efficiency and the bias for a loop of any size with a full account of the stress field in the loop region of influence. It is shown that the loop bias depends on the loop size, dislocation density and the interstitial to vacancy dilatation ratio. With increasing loop size its bias decreases or increases to the straight dislocation bias value if the dislocation density is low or high, respectively. The bias difference of loops of different sizes is shown to be the reason of a coexistence of vacancy and interstitial loops under irradiation. In the conventional case of the dislocation bias for interstitials, interstitial loops are expected to grow to larger sizes than vacancy loops, while in a special case of dislocation bias for vacancies, the opposite tendency is expected.

PACS: 61.72.Ji; 61.72.Qq; 61.80.Az

1. Introduction

Network dislocations and dislocation loops are usually the first observable extended defects in materials subjected to particle irradiation, and knowledge of the mechanisms controlling their evolution is essential for understanding of the mechanisms of irradiation damage. In this regard, the point defect diffusion into a straight dislocation and a dislocation loop with account of its stress field has been a subject of numerous investigations [1–9]. Most of the work is based on the analysis of the size effect, which is the principle elastic interaction between point defects and dislocations in most metals [1–7]. The main results of the work, in which the drift–diffusion problem is treated numerically within confines of linear elasticity theory and a point defect modeled as an isotropic center of dilatation or contraction [4–7], could be summarized as follows.

(1) Dislocation loops are biased sinks that attract self-interstitial atoms (SIAs) more strongly than vacancies.
(2) The loop absorption efficiency and bias depend on the loop radius and number density and do not depend on the loop character (vacancy or interstitial).
(3) For a fixed loop number density, as the loop radius increases its absorption efficiency and bias first decrease, then pass through the minimum and finally increase monotonically. The position of the

* Corresponding author. Tel./fax: +380 572 351781.
E-mail address: dubinko@ic.kharkov.ua (V.I. Dubinko).

0022-3115/$ - see front matter © 2004 Published by Elsevier B.V.
doi:10.1016/j.jnucmat.2004.07.034

minimum depends on the radius of the sink-free region, which models the effect due to sink–sink interaction.

(4) The absorption efficiency of a dislocation loop calculated from a model involving a surrounding spherical or cylindrical sink-free region of radius, R_{ext}, is a valid approximation only when the loop radius is smaller than $R_{ext}/2$.

In order to describe the dislocation structure evolution in the rate theory, it would be desirable to have analytical expressions for the loop absorption efficiency at any loop size. However, elastic interaction between PD and a dislocation loop is complicated and the resulting diffusion problem does not have an analytical solution. A finite-difference numerical method has been used that allows calculating the point defect current into a loop placed in a cylindrical [4,5] or spherical [6,7] reservoir, at which boundary a constant concentration of point defect is maintained.

A procedure of evaluation of the absorption efficiency of a dislocation loop from the point defect current needs some clarification. It is generally assumed that the steady-state current into the loop is proportional to the difference $\overline{C} - C^{eq}$, where $\overline{C}$ is the constant point defect concentration at the external boundary of the sink-free region and C^{eq} is the equilibrium concentration at the internal boundary, which corresponds to zero PD flux *in the absence of the stress field*. Then it is possible to determine a common factor, known as the absorption (or capture) efficiency, Z so that the point defect current per unit dislocation length, J, is given by $J = ZD(\overline{C} - C^{eq})$, where D is the point defect diffusivity.

As we will show in the present paper, this proportionality does not take place in a general case of PD diffusion in the dislocation stress field that changes *absorption* and *emission* efficiency of dislocations in a different way. The difference between the absorption and emission efficiency increases with decreasing the radius of the sink-free reservoir.

In the following section we will consider the point defect current into a straight dislocation. This problem has an exact analytical solution, which will help us to verify the numerical results and to define the *absorption* and *emission* efficiencies correctly.

In Section 3, we will use a finite-difference numerical method to calculate the point defect current into a dislocation loop placed in a *toroidal* sink-free reservoir, which is a more appropriate model for a dislocation loop than a spherical or cylindrical reservoir adopted in the previous models. It allows a direct evaluation of the point defect current into a loop of any size with a full account of the stress field in the loop region of influence. From this we will calculate the loop absorption and emission efficiencies and obtain analytical fitting functions describing their dependence on the loop radius sink density and material parameters.

In Section 4, we will calculate growth rates of dislocation loops in various irradiation environments in the effective medium approximation.

2. Bias of a straight dislocation

The change in the concentration of point defects (PD) due to diffusion in a stress gradient is given by

$$\frac{\partial C}{\partial t} = D\Delta C + \frac{D}{k_B T}\nabla E \nabla C + \frac{D}{k_B T} C \Delta E, \tag{1}$$

where D is the diffusion coefficient, C is the PD concentration, k_B is the Boltzmann's constant, T is the absolute temperature, $E(\vec{r})$ is the interaction energy of the point defect with the stress field. In the case of constant D and T, the introduction of dimensionless variables:

$$r \to \frac{r}{b}, \quad t \to \frac{t}{b^2} D, \quad E \to \frac{E}{k_B T},$$

where b is the Burgers vector, reduces Eq. (1) to the form

$$\frac{\partial C}{\partial t} = \Delta C + \nabla (C \nabla E). \tag{2}$$

$E(\vec{r})$ for an edge dislocation can be written in polar coordinates r, θ of the PD with respect to the dislocation line:

$$E(r,\theta) = \frac{\mu b (1+\nu)\Omega}{3\pi k_B T (1-\nu)} \frac{\sin\theta}{r}, \tag{3}$$

where b is the atomic spacing, μ is the shear modulus of the matrix, ν is the Poisson ratio, Ω is the PD relaxation volume per atomic volume, $\Omega = \Omega_v$ for vacancies and $\Omega = \Omega_i$ for interstitials.

The boundary condition at the dislocation core, $r = r_c$, is

$$C = C^{eq} \exp(-E(r_c,\theta)) \quad \text{at } r = r_c, \tag{4}$$

where C^{eq} is the equilibrium concentration corresponding to zero PD flux in the absence of the stress field. At the external boundary of the dislocation radius of influence, $r = R_{ext}$, the concentration is assumed to be equal to some average value, $\overline{C}$

$$C = \overline{C} \quad \text{at } r = R_{ext}. \tag{5}$$

In a steady-state one has from Eq. (2)

$$\Delta C + \nabla E \cdot \nabla C = 0 \tag{6}$$

since $E(r,\theta)$ is harmonic. The solution of Eq. (6) subject to the conditions (4) and (5) is based on the transformation of Eq. (6) into the equation for a new function, $\varphi(r,\theta)$:

$$\varphi(r,\theta) = C(r,\theta)\exp[E(r,\theta)/2] - C^{eq}\exp[-E(r,\theta)/2], \tag{7}$$

$$\Delta\varphi - \frac{1}{4}\varphi(\nabla E)^2 = 0 \tag{8}$$

subject to the boundary conditions

$$\varphi = 0 \quad \text{at } r = r_c, \tag{9}$$

$$\varphi = \overline{C}\exp[E(R_{ext},\theta)/2] - C^{eq}\exp[-E(R_{ext},\theta)/2] \ \text{ at } r = R_{ext}. \tag{10}$$

The boundary value at the dislocation core becomes zero while that at the external boundary now becomes spatially varying. The assumption has been made by many authors that the external boundary is sufficiently far away from the dislocation core, so that the interaction energy there is negligible, $E(R_{ext}) = 0$. *In this approximation*, one has instead of (10) a constant boundary condition:

$$\varphi = \overline{C} - C^{eq} \quad \text{at } r = R_{ext}. \tag{11}$$

The solution of Eq. (8) subject to conditions (9) and (11) is given by Margvelashvili and Saralidze [2], and it results in the following expressions for the PD current per the dislocation unit length, J_{str}, and the capture efficiency of a straight dislocation, Z_{str}:

$$J_{str} = Z_{str}D(\overline{C} - C^{eq}), \tag{12}$$

$$Z_{str} = \frac{2\pi I_0(L/2r_0)}{K_0(L/2R_{ext})I_0(L/2r_0) - K_0(L/2r_0)I_0(L/2R_{ext})}, \tag{13}$$

where $I_0(z)$ and $K_0(z)$ are the modified Bessel functions of zero order and L is the characteristic range of the interaction potential, which is proportional to the *absolute value* of the PD relaxation volume that is usually larger for SIAs than for vacancies:

$$L = \frac{\mu b(1+\nu)}{3\pi k_B T(1-\nu)} \mid \Omega \mid . \tag{14}$$

Note, that the PD current into a dislocation, given by Eq. (12) is proportional to $\overline{C} - C^{eq}$, which is in fact the result of the *approximate* boundary condition (11) rather than a general result. Only in this approximation, it is possible to determine a common factor, known as the *capture efficiency*, Z.

As we will show below, this proportionality does not take place in a general case of PD diffusion in the dislocation stress field.

Rauch and Simon [3] have found an analytical solution of Eq. (8) subject to the exact boundary condition (10), which yields the following expression for the PD current into a dislocation:

$$J_{str} = Z^a_{str}D\overline{C} - Z^e_{str}DC^{eq} = Z^a_{str}D(\overline{C} - C^{eq}_Z), \tag{15}$$

$$C^{eq}_Z = \frac{Z^e_{str}}{Z^a_{str}}C^{eq}, \tag{16}$$

$$Z^a_{str} = z_0(R_{ext}) + 2\sum_{n=1}^{\infty}(-1)^n z_n(R_{ext}), \tag{17}$$

$$Z^e_{str} = z_0(R_{ext}) + 2\sum_{n=1}^{\infty} z_n(R_{ext}), \tag{18}$$

where

$$z_n(R_{ext}) = \frac{2\pi I_n(L/2r_0)I_n(L/2R_{ext})}{I_n(L/2r_0)K_n(L/2R_{ext}) - I_n(L/2R_{ext})K_n(L/2r_0)}, \tag{19}$$

where $I_m(z)$ and $K_m(z)$ are the modified Bessel functions of the nth order. The factors Z^a_{str} and Z^e_{str} can be called *absorption* and *emission* efficiencies, respectively, and they are not generally equal. Hence, in contrast to the approximate solution (12), one has $J_{str} \propto \overline{C} - C^{eq}_Z$, and so when $\overline{C} = C^{eq}_Z$, there will be no net flow into the dislocation. It means that the dislocation stress field changes the equilibrium PD concentration by a factor Z^e_{str}/Z^a_{str}, which depends on the radius of the dislocation region of influence R_{ext} determined by the total sink strength of the system, k^2_{tot} [10]:

$$R_{ext}(k_{tot}) = \sqrt{\frac{Z^a_{str}(k_{tot})}{\pi k^2_{tot}}}. \tag{20}$$

Fig. 1 shows that the approximation (12) can be justified only in the case of low sink density ($\leqslant 10^9$ cm^{-2}) when $L/2R_{ext}$ is sufficiently small so that $Z^e_{str}/Z^a_{str} \approx 1$, $C^{eq}_Z \approx C^{eq}$. At higher sink densities one has $C^{eq}_Z > C^{eq}$, and so it is not generally correct to follow the conventional scheme and define a common 'capture' efficiency as the ratio

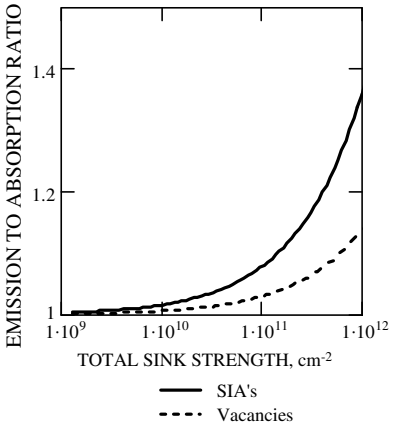

Fig. 1. Ratio of emission to absorption efficiency, Z^e_{str}/Z^a_{str} for a straight dislocation vs. total sink strength.

$$Z^{\mathrm{com}} = \frac{J}{D(\overline{C} - C^{\mathrm{eq}})} \tag{21}$$

since the result of such definition will depend on the PD supersaturation, $S = (\overline{C} - C^{\mathrm{eq}})/C^{\mathrm{eq}}$, as will be shown below.

Substituting (15) into (21) one obtains for the common 'capture' efficiency the expression, which depends on the supersaturation:

$$Z^{\mathrm{com}}_{\mathrm{str}}(S) = \frac{J_{\mathrm{str}}}{D(\overline{C} - C^{\mathrm{eq}})} = \frac{Z^{\mathrm{a}}_{\mathrm{str}}\overline{C} - Z^{\mathrm{e}}_{\mathrm{str}}C^{\mathrm{eq}}}{\overline{C} - C^{\mathrm{eq}}} = \frac{Z^{\mathrm{a}}_{\mathrm{str}}(S+1) - Z^{\mathrm{e}}_{\mathrm{str}}}{S}. \tag{22}$$

Such dependence is a result of incorrect definition and it can be misleading, as it is demonstrated in Fig. 2, which shows the straight dislocation bias dependence on the sink density. Two different definitions are compared, namely, the common $B^{\mathrm{com}}_{\mathrm{str}}$ and the absorption dislocation bias, $B^{\mathrm{a}}_{\mathrm{str}}$, is defined as follows:

$$B^{\mathrm{com}}_{\mathrm{str}} = 1 - Z^{\mathrm{com}}_{\mathrm{str,v}}/Z^{\mathrm{com}}_{\mathrm{str,i}}, \quad B^{\mathrm{a}}_{\mathrm{str}} = 1 - Z^{\mathrm{a}}_{\mathrm{str,v}}/Z^{\mathrm{a}}_{\mathrm{str,i}}, \tag{23}$$

where the subscripts i and v correspond to SIAs and vacancies, respectively. Dashed curve corresponds to approximate analytical solution (13), solid curve – to the exact analytical solution (17) for the absorption bias, dotted curve – to the exact solution (22) for the common 'bias', circles and squares correspond to the absorption and common biases obtained from the PD current calculated numerically for a dislocation placed in the cylindrical reservoir (the calculation procedure is similar to that described in Appendix A).

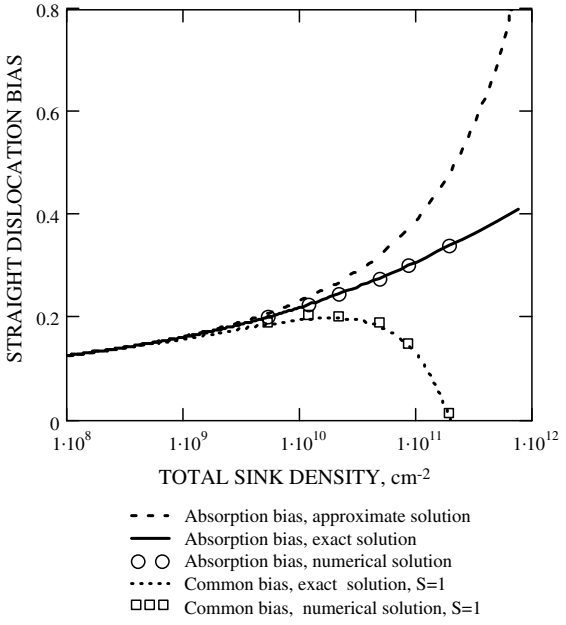

Fig. 2. Dislocation bias dependence on the sink density.

Only in the case of high supersaturation, $S \gg 1$, the common bias coincides with the exact absorption bias, which does not depend on S and increases monotonously with increasing sink density. Note that the exact solution (17) increases less steeply than the approximate one (13).

At low supersaturation, $S = 1$, the common 'bias' starts to decrease with increasing sink density above 2×10^{10} cm^{-2} and comes to zero at about 2×10^{11} cm^{-2}, i.e. it behaves completely different as compared to the absorption bias.

From the methodical point of view, the discrepancy between the common and absorption bias shows the importance of a correct formulation of the bias evaluation scheme. To avoid confusion, we will define *absorption* and *emission* efficiencies, Z^{a} and Z^{e}, which should be determined from the solution of diffusion problem *separately*:

$$Z^{\mathrm{a}} = \frac{J(C^{\mathrm{eq}} = 0)}{D\overline{C}}, \quad Z^{\mathrm{e}} = \frac{J(\overline{C} = 0)}{DC^{\mathrm{eq}}}. \tag{24}$$

This definition will be used in the following section dealing with evaluation of the loop bias from a numerical solution of the diffusion problem.

3. Bias of SIA and vacancy dislocation loops

The problem of three-dimensional diffusion of point defects in a stress field of the dislocation loop does not have an exact analytical solution, because of the defect interaction complexity, so the numerical technique is used. We have used the numerical solution of the steady-state diffusion equation [6] for the calculation of the loop bias factor.

We have considered the migration of point defects into a dislocation loop with a radius R placed in a *toroidal reservoir* of the larger radius, R_{ext}, coaxial to the dislocation loop, at which external boundary a constant concentration $\overline{C}$ is maintained. The internal boundary is the toroidal surface of radius r_{c}, at which the equilibrium concentration is assumed:

$$C = C^{\mathrm{eq}} \exp(-E(r_0, \theta)) \quad \text{at } r = r_{\mathrm{c}}, \tag{25}$$

where C^{eq} is the equilibrium concentration corresponding to zero PD flux in the absence of the stress field.

For the definition of the dislocation core radius r_{c} we used the following equation

$$\mathrm{grad}\left.\frac{E(r)}{k_{\mathrm{B}}T}\right|_{r=r_{\mathrm{c}}} = \frac{1}{b} \tag{26}$$

according to [4]. The surface defined by Eq. (26) encloses a region in which a newly arrived PD may be considered to be absorbed. When r_{c} is defined like that it depends on the PD dilatation volume, temperature and loop radius. For a straight dislocation, the definition (26)

results in the following expression for the dislocation core radius:

$$r_c|_{R\to\infty} = (bL)^{1/2}. \quad (27)$$

The calculation scheme is described in Appendix A. Calculations are made for zirconium at $T = 573$ K, the material parameters are given in Table 1. We have calculated *absorption* and *emission* efficiencies, Z^a and Z^e, which are determined by Eq. (24).

The *toroidal* reservoir, in contrast to *cylindrical* or *spherical* reservoir adopted in the previous models [4,6] allows a direct evaluation of the PD current for a loop of any size with a full account of the stress field in the loop region of influence. In Fig. 3, numerical results of Z^a calculation for spherical and toroidal reservoir are compared in the case of $R_{ext} = 78b$, which corresponds to the dislocation density, $\rho_d \approx 1/\pi R_{ext}^2 \approx 5\times10^{10}$ cm^{-2}. It can be seen that in the spherical reservoir, the influence of external boundary starts already for $R > 0.25R_{ext}$ resulting in a sharp increase of Z^a. In contrast to that, in the toroidal reservoir, Z^a passes through the minimum at $R \approx 0.5R_{ext}$ and then steadily increases to the straight dislocation value Z^a_{str}.

Table 1
Material parameters of Zr used in calculations

Parameter	Value
Matrix shear modulus, μ, GPa	33
Poisson ratio, ν	0.33
Burgers vector, b, m	3.23×10^{-10}
Atomic volume of the host lattice, ω, m^{-3}	2.36×10^{-29}
Interstitial relaxation volume, Ω_i [7]	1.2ω; 0.3ω
Vacancy relaxation volume, Ω_v [7]	-0.6ω
Recombination rate constant, β_r, m^{-2}	1.72×10^{20}
Vacancy formation energy, E_{vf}, eV	1.9
SIA formation energy, E_{if}, eV	4.04
Diffusion coefficient of interstitials, D_i, m^2/s	$10^{-7}\exp(-0.3\ \text{eV}/k_BT)$
Diffusion coefficient of vacancies, D_v, m^2/s	$2\times10^{-5}\exp(-1.104\ \text{eV}/k_BT)$

The *absorption* bias evaluated using Eq. (24) *does not depend on the loop type*, in agreement with the previous models. With increasing loop size its bias decreases or increases to the straight dislocation bias if the dislocation density is low or high, respectively (Fig. 4).

On the other hand, the sink–sink interaction breaks the symmetry between SIA and vacancy loops in respect to the PD *emission*, as shown in Fig. 5. Emission efficiency of vacancies *is larger* for SIA loops and *smaller* for vacancy loops than absorption efficiency. It can be seen that at sufficiently small R or large R_{ext} the absorption and emission efficiencies coincide and the difference between them becomes significant for relatively large loops and high sink density. This effect favors the growth of *both* SIA and vacancy loops of sufficiently large sizes ranging from *tens to hundreds nanometers* depending on the sink density.

In order to use the numerical results in the rate theory calculation we obtained the following analytical fitting formulas for absorption and emission efficiencies as the functions of the loop radius and type, sink density (via R_{ext} and Eq. (20)), PD dilatation volume and temperature:

$$Z^a(R,R_{ext},\Omega,T) = Z^a_{str}(R_{ext},\Omega,T) + \frac{3.6\cdot L(\Omega,T)^{0.255} - Z^a_{str}(R_{ext},\Omega,T)}{(R/b)^{2/3}+0.2}. \quad (28)$$

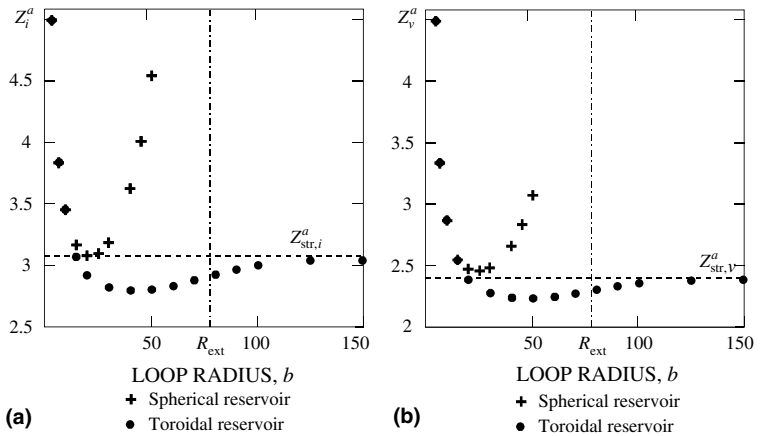

Fig. 3. Interstitial and vacancy absorption efficiency, Z^a_i (a) and Z^a_v (b) as a function of the loop radius for toroidal and spherical reservoir, calculated for $R_{ext} = 78b$. Dashed lines represent absorption efficiencies of straight dislocation, according to Eq. (17).

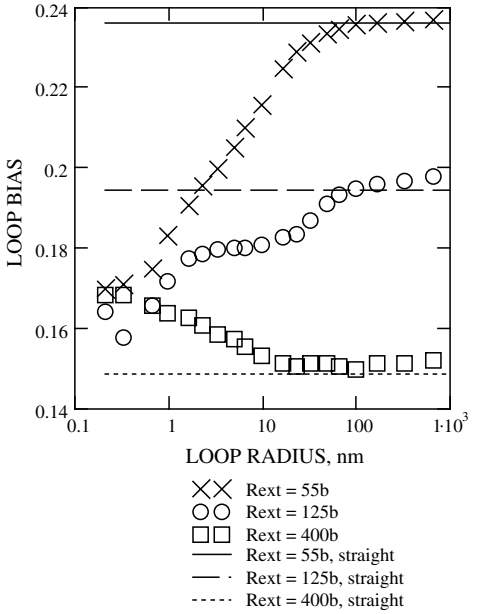

Fig. 4. Absorption bias as a function of the loop radius for $\rho_d \approx 10^{11}$ cm^{-2} ($R_{ext} = 55b$), $\rho_d \approx 2\times10^{10}$ cm^{-2} ($R_{ext} = 125b$) and $\rho_d \approx 2\times10^{9}$ cm^{-2} ($R_{ext} = 400b$). The lines correspond to analytical calculations for straight dislocations.

$$Z^e(R,R_{ext},\Omega,T) = Z^a(R,R_{ext},\Omega,T) \times \left[1+\frac{Z^e_{str}(R_{ext},\Omega,T)-Z^a_{str}(R_{ext},\Omega,T)}{Z^a(R,R_{ext},\Omega,T)}\cdot\frac{1}{1+5R_{ext}/R}\right] \times \left\{1+\frac{\pm L(\Omega,T)+180b^2/R_{ext}}{R+1.5R_{ext}}\left[1+\tanh\left(\frac{10R}{3R_{ext}}-3\right)\right]\right\}. \quad (29)$$

The absorption efficiency does not depend on the loop or PD type and depends only on the absolute value of the PD dilatation volume. The emission efficiency depends on the loop and PD type: the sign '+' in Eq. (29) is for Z^e_{Vi} and Z^e_{SIAv}, the sign '−' is for Z^e_{Vv} and Z^e_{SIAi}, where subscripts 'V' and 'SIA' correspond to vacancy and SIA loops, 'v' and 'i' correspond to vacancies and SIA's.

The obtained formulas are valid for any loop size and they coincide with analytical expressions for straight dislocations at $R \to \infty$. Figs. 6 and 7 show comparison of the fitting formulas with numerical results for the loop absorption bias and vacancy emission efficiencies in the case dislocation bias for SIA's ($\Omega_i/|\Omega_v| = 2$).

The obtained formulas allow us to consider an interesting case of the dislocation bias for *vacancy absorption*, which can be realized in those materials where SIAs have smaller dilatation volume than vacancies: $\Omega_i/|\Omega_v| < 1$. In this case, the loop bias for vacancies, $Z^a_v/Z^a_i - 1 > 0$, is an increasing or decreasing function of the loop size, if the dislocation density is high or low, respectively, as shown in Fig. 8.

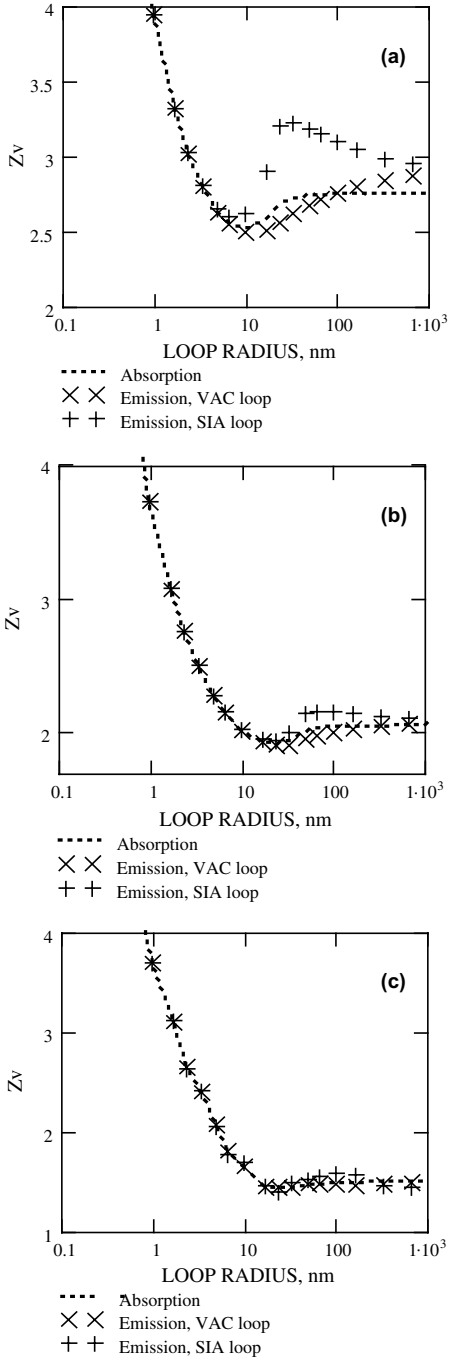

Fig. 5. Vacancy absorption and emission efficiencies as the functions of the loop radius for (a) $\rho_d \approx 10^{11}$ cm^{-2} ($R_{ext} = 55b$), (b) $\rho_d \approx 2\times10^{10}$ cm^{-2} ($R_{ext} = 125b$), and (c) $\rho_d \approx 2\times10^{9}$ cm^{-2} ($R_{ext} = 400b$).

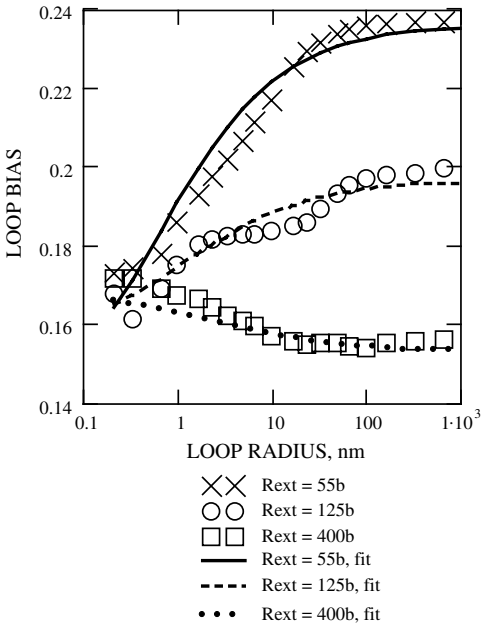

Fig. 6. Absorption bias for SIA's ($\Omega_i/|\Omega_v| = 2$) as a function of the loop radius for $\rho_d \approx 10^{11}$ cm^{-2} ($R_{ext} = 55b$), $\rho_d \approx 5\times10^{10}$ cm^{-2} ($R_{ext} = 78b$) and $\rho_d \approx 2\times10^{9}$ cm^{-2} ($R_{ext} = 400b$).

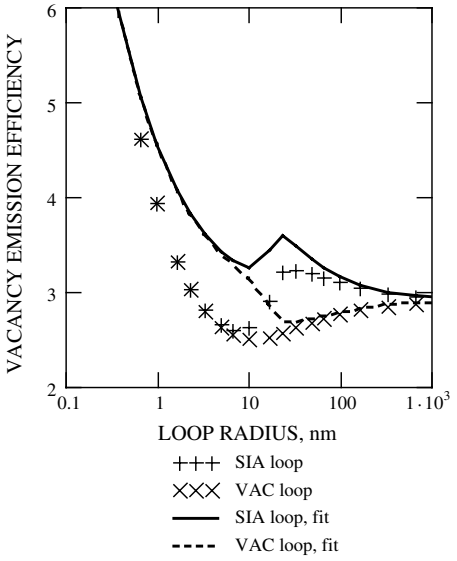

Fig. 7. Vacancy emission efficiency Z_v^e as a function of the loop radius for $\rho_d \approx 10^{11}$ cm^{-2} ($R_{ext} = 55b$).

4. Growth rates of SIA and vacancy dislocation loops

Growth rates of dislocation loops are determined in the rate theory by the difference between the net currents of SIA's and vacancies:

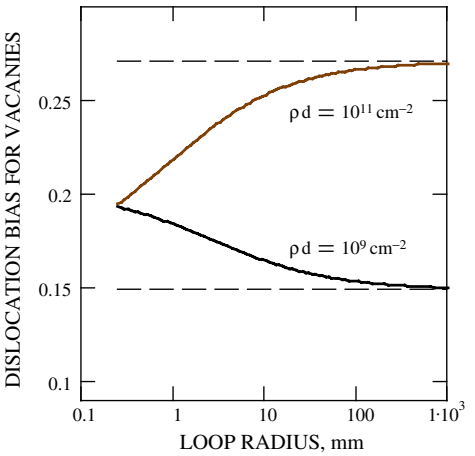

Fig. 8. Bias of a dislocation loop for *vacancy absorption* ($\Omega_i/|\Omega_v| = 0.5$) as a function of the loop radius at different dislocation densities. Solid curves correspond to the loop bias, dashed lines – to the straight dislocation bias.

$$\frac{dR_{VL}}{dt} = \frac{1}{b}\left[Z_v^a D_v\left(\overline{C}_v - \frac{Z_{Vv}^e}{Z_v^a}C_{Vv}^{eq}\right) - Z_i^a D_i\left(\overline{C}_i - \frac{Z_{Vi}^e}{Z_i^a}C_{Vi}^{eq}\right)\right], \tag{30}$$

$$\frac{dR_{SIAL}}{dt} = \frac{1}{b}\left[Z_i^a D_i\left(\overline{C}_i - \frac{Z_{SIAi}^e}{Z_i^a}C_{SIAi}^{eq}\right) - Z_v^a D_v\left(\overline{C}_v - \frac{Z_{SIAv}^e}{Z_v^a}C_{SIAv}^{eq}\right)\right], \tag{31}$$

where subscripts 'V' and 'SIA' correspond to vacancy and SIA loops, 'v' and 'i' correspond to vacancies and SIA's, C^{eq} is the *field free* local equilibrium concentration of PD's at the dislocation loop core, which can also depend on the loop type and radius, $\overline{C}$ is the mean concentrations of PD's in the bulk, which are determined by the rate equations:

$$\frac{d\overline{C}}{dt} = K + K^e - k^2 D\overline{C} - \beta_r(D_v + D_i)\overline{C}_v\overline{C}_i, \tag{32}$$

where K is the generation rate of Frenkel pairs in the bulk, K^e is the emission rate of Schottky defects from extended defects, k^2 is the microstructure sink strengths, β_r is the constant of the bulk recombination of PD's.

Fig. 9 shows dislocation loop growth rates calculated by Eqs. (30) and (31) in the case of dislocation *bias for SIA absorption*, $\Omega_i/|\Omega_v| = 2$ at a temperature sufficiently low for any significant thermal vacancy emission. It is seen that the growth rates of vacancy and interstitial loops are always opposite in sign. At low initial dislocation density, the bias of dislocation loops is larger than the straight dislocation bias (Fig. 6) implying that SIA-loops will grow while vacancy loops shrink (Fig. 9(a)). Formation of a microstructure made up of SIA loops increases the total dislocation density, which

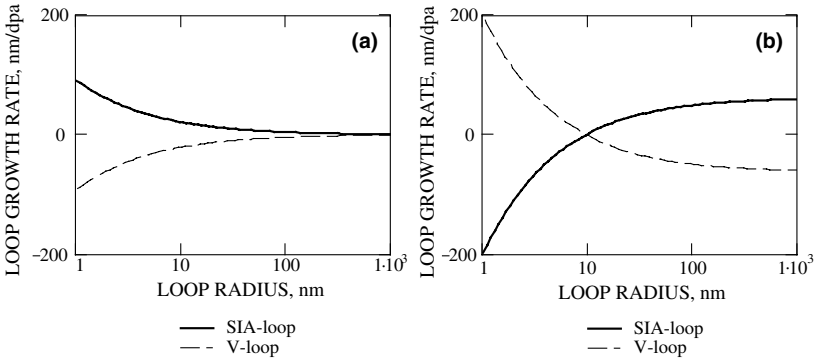

Fig. 9. Dislocation loop growth rates at $K = 10^{-8}$ dpa/s, $T = 573$ K in the case of dislocation *bias for SIA absorption*, $\Omega_i/|\Omega_v| = 2$. (a) $\rho_d = 10^9$ cm^{-2}, no loops; (b) $\rho_d = 10^9$ cm^{-2}, mean loop radius $R_L = 10$ nm and the number density $N_L = 10^{16}$ cm^{-3}.

results in alteration of the character of the size dependence of loop bias, i.e. the loop bias becomes an increasing function of the loop radius (Fig. 6). Consequently, there will be a net flow of vacancies to the smaller loops and a net flow of SIAs to larger loops (Fig. 9(b)). The intersection point of the loop growth rates determines the critical loop size at which the loop growth rate is zero. Below this size, the growth rate is positive for vacancy loops and above this size, it is positive for SIA loops. For this reason, the growing vacancy loops will accumulate at the intersection point in the size space. Simultaneously, the SIA loop growth beyond the critical size is enhanced so that the larger loops may grow at the expense of the smaller ones. This is a characteristic example of the radiation-induced coarsening (RIC) of dislocation loops, which is similar to the RIC of voids [10], since in both cases, the bias differential is a driving force of the coarsening.

In the case of dislocation *bias for vacancy absorption*, $\Omega_i/|\Omega_v| = 0.5$, interstitial and vacancy loops change places. Now vacancy loops will grow at a low initial dislocation density (Fig. 10(a)). At the high loop density, there will be a net flow of SIA's to the smaller loops and a net flow of vacancies to larger loops (Fig. 10(b)). Accordingly, the growing SIA loops will accumulate at the intersection point in the size space, while the larger vacancy loops will grow due to the RIC mechanism.

5. Discussion

According to present results, in the conventional case of the dislocation bias for SIA absorption, $\Omega_i/|\Omega_v| > 1$, there will be a net flow of vacancies to the smaller loops and a net flow of SIAs to larger loops, which provides a sufficient condition for the simultaneous growth of both vacancy and interstitial loops on the same habit plane observed in Zr, Ti and Mg [11–13]. However, according to this model, the vacancy loops should be smaller than the adjacent interstitial loops, and this is not always confirmed by experimental data. In some cases the opposite is true, e.g. **a**-type interstitial loops formed in electron irradiated Mg were consistently smaller (about 100 nm in diameter) than the vacancy loops (about 500 nm in diameter) [12].

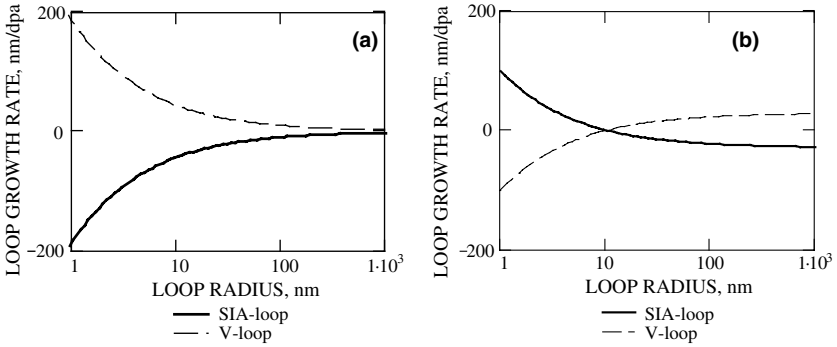

Fig. 10. Dislocation loop growth rates at $K = 10^{-8}$ dpa/s, $T = 573$ K in the case of dislocation *bias for vacancy absorption*, $\Omega_i/|\Omega_v| = 0.5$. (a) $\rho_d = 10^9$ cm^{-2}, no loops; (b) $\rho_d = 10^9$ cm^{-2}, mean loop radius $R_L = 10$ nm and the number density $N_L = 10^{16}$ cm^{-3}.

Wolfer and Si-Ahmed [9] proposed that non-linear elasticity theory might produce an intrinsic bias differential between vacancy and interstitial loops. This effect decreases rapidly with increasing loop size and so it can hardly be applied to explain the growth of large vacancy loops.

An alternative theory was suggested by Woo [8] who considered point defect diffusion into an *infinitesimal* edge dislocation loop including the effects of the saddle-point shape anisotropy of point defects. The loop bias was found to depend on the loop nature and the point defect shape at the saddle point but its dependence on the loop size (especially for large loops) remained unclear.

The present results provide an alternative mechanism for the vacancy loops growth to sizes exceeding the size of SIA loops, which can be realized in those materials where SIAs have smaller dilatation volume than vacancies: $\Omega_i/|\Omega_v| < 1$. In this case, there will be a net flow of vacancies to the larger vacancy loops and a net flow of SIAs to smaller SIA loops. This case may be of a special interest for Zr alloys, in which SIAs are known to have an unusually small dilatation volume and which are rather reluctant to the void formation as compared to other metals [13].

Another possible mechanism for the simultaneous growth of *large* SIA and vacancy loops is based on a modified emission efficiency of vacancies, such that the vacancy emission from large V-loops is less than that from SIA-loops. The practical significance of this mechanism depends crucially on the ratio of the *vacancy emission rate* from sinks to the Frenkel production rate in the bulk. If the vacancy emission is due to thermal fluctuations only then it can be significant only at sufficiently high temperatures. If a radiation-induced vacancy emission from dislocations is involved [14], then it can be significant at lower temperature range as well.

We also note that in the high sink density case, one should take into account the effects due to internal stress from other loops. However, such calculations are outside the scope of the present paper.

6. Summary

- The dislocation loop absorption and emission efficiencies for PD have been calculated numerically as functions of the loop size and type, the total sink strength, temperature and the PD dilatation volume.
- The loop bias for SIA or vacancy *absorption* depends on the loop size, dislocation density, PD dilatation ratio, $\Omega_i/|\Omega_v|$, and does not depend on the loop type. With increasing loop size its bias decreases or increases to the straight dislocation bias value if the dislocation density is low or high, respectively.
- A coexistence of vacancy and interstitial loops is possible due to a bias difference of loops of different sizes. In the conventional case of the dislocation bias for SIA's, $\Omega_i/|\Omega_v| > 1$, SIA loops are expected to grow to larger sizes than vacancy loops, while in a special case of dislocation bias for vacancies, $\Omega_i/|\Omega_v| < 1$, the opposite tendency is expected.
- Emission efficiency of vacancies *is larger* for SIA loops and *smaller* for vacancy loops, and the difference between them increases with increasing sink density. This effect favors the growth of *both* SIA and vacancy loops of sufficiently large sizes ranging from tens to hundreds nanometers depending on the sink density. The practical significance of this effect depends on the ratio of the *vacancy emission rate* from sinks to the Frenkel pair production rate in the bulk.
- In order to use the numerical results in the rate theory calculation, analytical fitting formulas for absorption and emission efficiencies have been obtained as the functions of the loop radius and type, sink density, PD dilatation volume and temperature.

Acknowledgements

This study has been supported by the AECL, Canada via the STCU partner grant #P-049. We would also like to acknowledge Dr M. Griffiths for many useful discussions.

Appendix A. Numerical calculation scheme

We have considered the migration of point defects into a dislocation loop with a radius R placed in a reservoir, at which boundary a constant concentration $\overline{C}$ is maintained. Two cases have been considered: (i) a spherical reservoir of a radius R_{ext} (Fig. 11), and (ii) a toroidal reservoir coaxial to the dislocation loop (Fig. 12). The internal boundary in both cases is the toroidal surface, at which the equilibrium concentration is assumed. Let us introduce the cylindrical coordinate system, where z-axis is orthogonal to the dislocation loop plane. Note that the diffusion field has rotational symmetry about the z-axis. Taking into account the reflection symmetries, the corresponding boundary value problem can be formulated with reference to Figs. 11 and 12.

For the spherical reservoir (Fig. 11) and toroidal reservoir at $R < R_{ext}$ (Fig. 12(b)), the diffusion–drift equation is given by Eq. (2) in the region bounded by the surfaces 0A, AB, BC, CD, D0. For the toroidal reservoir at $R > R_{ext}$ (Fig. 12(a)), the diffusion–drift equation is given by Eq. (2) in the region bounded by the surfaces DA, AB, BC, CD. The boundary conditions are given

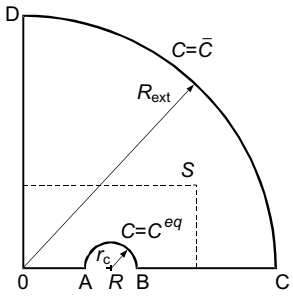

Fig. 11. Disposition of the co-ordinate system used for the spherical reservoir.

by Eq. (4) at the dislocation core, and by Eq. (5) at the external boundary, at the 0A and BC

$$\frac{\partial C}{\partial z} = 0 \tag{A.1}$$

and at the $r = 0$

$$\frac{\partial C}{\partial r} = 0. \tag{A.2}$$

To circumvent a strong angular dependence of the concentration at the dislocation core (the boundary condition (4)) we introduce the following transformation [15], which differs slightly from Eq. (7), which was used for the analytical calculations:

$$\psi(r,z) = C(r,z)\exp[E(r,z)]. \tag{A.3}$$

In terms of ψ, the diffusion equation takes the form

$$\frac{\partial \psi}{\partial t} = \frac{\partial^2 \psi}{\partial r^2} + \frac{\partial^2 \psi}{\partial z^2} + \left(\frac{1}{r} - \frac{\partial E}{\partial r}\right)\frac{\partial \psi}{\partial r} - \frac{\partial E}{\partial z}\frac{\partial \psi}{\partial z}. \tag{A.4}$$

The boundary conditions are

$$\psi(r,z) = \psi_{\text{ext}}(r,z) = \overline{C}\exp[E(R_{\text{ext}})] \quad \text{at } r = R_{\text{ext}}, \tag{A.5}$$

$$\psi(r,z) = \psi_0 \quad \text{at } r = r_c, \tag{A.6}$$

$$\frac{\partial \psi}{\partial z} = 0, \quad \text{at the 0A and BC}, \tag{A.7}$$

$$\frac{\partial \psi}{\partial r} = 0, \quad \text{at the 0D}. \tag{A.8}$$

For a dislocation loop, the drift field E has been calculated by Bastecka and Kroupa [16]. In dimensionless variables it is given by

$$E(r,z) = -\frac{\mu b(1+\nu)\Omega}{3\pi k_B T(1-\nu)}\frac{1}{\sqrt{(r+R)^2+z^2}} \times \left\{\frac{R^2 - r^2 - z^2}{(R-r)^2 + z^2}E_e(k) + K_e(k)\right\}, \tag{A.9}$$

where $E_e(k)$ and $K_e(k)$ are the complete elliptic integrals of the first and second kind, respectively. The argument k is defined by

$$k = \frac{4rR}{(r+R)^2 + z^2}. \tag{A.10}$$

The absorption and emission efficiencies of the dislocation loop, according to Eq. (24), are defined as

$$Z^a_{\alpha,S} = \frac{1}{2\pi R\overline{C}} I_{\alpha,S}|_{C^{eq}=0} = \frac{1}{2\pi R\overline{C}}\int_L e^{-E_z}\nabla\psi_\alpha \, dS, \tag{A.11}$$

$$Z^e_{\alpha,S} = \frac{1}{2\pi RC^{eq}} I_{\alpha,S}|_{\overline{C}=0} = \frac{1}{2\pi RC^{eq}}\int_L e^{-E_z}\nabla\psi_\alpha \, dS, \tag{A.12}$$

where $I_{\alpha,S}$ is the point-defect flux into the loop and S is any closed surface surrounding the loop, α = i, v.

We need a steady-state solution of Eq. (A.4), so we have considered a reduced form of Eq. (A.4) without the time derivative:

$$\frac{\partial^2 \Psi}{\partial r^2} + \frac{\partial^2 \Psi}{\partial z^2} + \left(\frac{1}{r} - \frac{\partial E}{\partial r}\right)\frac{\partial \Psi}{\partial r} - \frac{\partial E}{\partial z}\frac{\partial \Psi}{\partial z} = 0. \tag{A.13}$$

The boundary value problem Eq. (A.13) and Eqs. (A.5)–(A.8) was solved numerically by a finite-difference method [6].

It can be shown [7] that the use of the approximate boundary condition

$$\Psi(r,z) = \Psi_{\text{ext}}(r,z) = \overline{C} \quad \text{at } r = R_{\text{ext}}, \tag{A.14}$$

which corresponds to zero stress field at the external boundary in Eq. (A.5), would result in equal absorption and emission efficiencies, similar to the straight dislocation

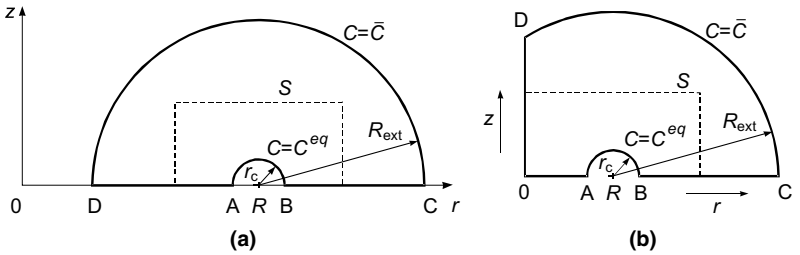

Fig. 12. Disposition of the co-ordinate system used for toroidal reservoir: (a) $R > R_{\text{ext}}$, (b) $R < R_{\text{ext}}$.

case. In this case, the emission efficiency does not depend on the loop type, in agreement with previous results [7].

When the exact boundary condition (Eq. (A.5)) is used, emission efficiency is different from the absorption efficiency and depends on the loop type (Fig. 5).

References

[1] F.S. Ham, J. Appl. Phys. 30 (1959) 915.
[2] I.G. Margvelashvili, Z.K. Saralidze, Fiz. Tverd. Tela. 15 (1973) 2665.
[3] H. Rauch, D. Simon, Phys. Sta. Sol. (a) 46 (1978) 499.
[4] W.A. Coghlan, in: Proceedings of the Computer Simulation for Materials Applications, 1976, p. 166.
[5] W.A. Coghlan, M.H. Yoo, Trans. Am. Nucl. Soc. 22 (1977) 330.
[6] C.H. Woo, W.S. Liu, M.S. Wuschke, AECL-6441, 1979.
[7] C.H. Woo, J. Nucl. Mater. 98 (1981) 279.
[8] C.H. Woo, J. Nucl. Mater. 107 (1982) 20.
[9] W.G. Wolfer, A. Si-Ahmed, Phys. Lett. 76A (1980) 341.
[10] V.I. Dubinko, P.N. Ostapchuk, V.V. Slezov, J. Nucl. Mater. 161 (1989) 239.
[11] M. Griffiths, Philos. Mag. A 63 (1991) 835.
[12] M. Griffiths, J. Nucl. Mater. 205 (1993) 225.
[13] M. Griffiths, J. Nucl. Mater. 159 (1988) 190.
[14] V.I. Dubinko, arXiv/cond-mat/0212154.
[15] W.G. Wolfer, M. Ashkin, J. Appl. Phys. 46 (1975) 547, 47 (1976) 791.
[16] J. Bastecka, F. Kroupa, Chechoslov. J. Phys. [B] 14 (1964) 443.